

Appearance of classical Mixmaster Universe from the No-Boundary Quantum State

Kazuya Fujio* and Toshifumi Futamase†

Astronomical Institute, Tohoku University, Sendai 980-8578, Japan

(Dated: October 26, 2018)

We investigate the appearance of the classical anisotropic universe from the no-boundary quantum state according to the prescription proposed by Hartle, Hawking and Hertog. Our model is homogeneous, anisotropic, closed universes with a minimally coupled scalar field and cosmological constant. We found that there are an ensemble of classical Lorentzian histories with anisotropies and experience inflationary expansion at late time, and the probability of histories with anisotropies are lower than isotropic histories. Thus the no-boundary condition may be able to explain the emergence of our universe. If the classical late time histories are extended back, some become singular by the existence of initial anisotropies with large accelerations. However we do not find any chaotic behavior of anisotropies near the initial singularity.

I. INTRODUCTION

Quantum cosmology is one of the most ambitious subject in physics. Its aim is to treat the universe itself by quantizing spacetime and to explain the creation of universe. We have not been able to treat the subject fully satisfactory because we do not have a complete theory of quantum gravity. However we do have very interesting approaches to the subject using best knowledge of our understanding of general relativity and quantum field theory. One is the quantum cosmology based on canonical quantization of general relativity. By using Hamiltonian formulation of general relativity and regarding 3-metric and its conjugate as fundamental operators, one can obtain Schrodinger like equation on the space of 3-metric(superspace), known as *Wheeler-DeWitt equation* $\hat{H}\Psi(q^A) = 0$, where the q^A are a set of coordinates for minisuperspace and $\Psi(q^A)$ is interpreted as wave function of the universe. By restricting the spacetime to homogeneous and isotropic(called minisuperspace), Wheeler-DeWitte equation greatly simplifies and an interesting idea for the origin of the universe have been proposed[1]. However, nobody knows how to calculate the probability of specific universe in this approach, and there are some problems e.g. the problem of time. There has been some progress in the past 10 years or so in this approach based on loop quantum gravity(e.g. Ashtekar [2], Bojowald [3]).

The another approach is based on the path integral quantization and is called no-boundary proposal for the wave function of the universe[4]. In this approach the wave function of the universe is defined by summing all Euclidean compact geometry weighted by exponential of action $\exp(-I)$ without boundary. As Hawking said ; *the boundary condition of the universe are that has no boundary* (Hartle & Hawking [4], Hawking [5]). Accord-

ing to this proposal the origin of the quasiclassical realm from the no-boundary proposal for the quantum state of the universe has been discussed by Hartle, Hawking and Hertog [6] in a class of minisuperspace models with homogeneous, isotropic closed spacetime geometries. They argued that a wave function with the semiclassical form

$$\Psi(q^A) = A(q^A)e^{iS(q^A)/\hbar} \quad (1)$$

in some region of minisuperspace predicts an ensemble of classical trajectories provided that $S(q^A)/\hbar$ is rapidly varying and $A(q^A)$ is slowly varying. It was shown that the complex solutions(metrics) of Euclidean Einstein equations that extremize the Euclidean action are distinct from the real Lorentzian classical metrics for which they provide the probabilities, and the probabilities for classical histories derived from the no-boundary wave function do define a measure on classical phase space.

It will be very interesting to see if it is possible to apply their method to more general class of minisuperspace. This is the aim of the paper. Namely we investigate the emergence of classical universes with anisotropy according to the prescription proposed by HHH. We consider the Bianchi type IX spacetime which is homogeneous but not isotropic, with a minimally coupled scalar field moving in a quadratic potential and cosmological constant. Quantum cosmology of Bianchi type IX model has been studied using Wheeler-DeWitte equation. For example, Battisti et al. [7] investigated the situation where the isotropic scale factor is considered as intrinsically different variable from anisotropies. Namely, they regarded the scale factor as time-parameter, and showed that the wave function of the universe is spread over all values of anisotropy near the cosmological singularity. However, it is also shown that the wave function asymptotically peaked around the isotropic configuration when the universe grows large. We will also find that the universe approaches isotropic configuration, but possible range of anisotropy near the bounce or singularity is very restricted unlike their result, but is consistent with the prediction by loop quantum cosmology[15].

*fujio@astr.tohoku.ac.jp

†tof@astr.tohoku.ac.jp

The organization of the paper is as follows. We briefly review mixmaster universe in Sec. II and explain the condition of classicality according to HHH in Sec. III. Then we calculate the wave function of our model and applies the prescription of HHH in Sec. IV. The numerical results are shown in Sec. V. Finally summary and some discussion will be given in Sec. VI.

II. MIXMASTER UNIVERSE

In this section we briefly review Bianchi type IX model. The geometry of Bianchi type IX model may be written as

$$ds^2 = -N^2 dt^2 + e^{2\alpha} (e^{2\beta})_{ij} \sigma^i \sigma^j \quad (2)$$

where N is the lapse function and β_{ij} represent spacetime anisotropy. The 1-forms σ^i are defined by

$$\begin{aligned} \sigma^1 &= \cos \psi d\theta - \cos \psi \sin \theta d\phi \\ \sigma^2 &= \sin \psi d\theta - \cos \psi \sin \theta d\phi \\ \sigma^3 &= d\psi + \cos \theta d\phi \end{aligned} \quad (3)$$

N, α, β_{ij} are functions of time t . The anisotropy variables β_{\pm} are parametrized as follows;

$$\begin{aligned} \beta_{11} &= \beta_+ + \sqrt{3}\beta_- \\ \beta_{22} &= \beta_+ - \sqrt{3}\beta_- \\ \beta_{33} &= -2\beta_+ \end{aligned} \quad (4)$$

Thus the dynamical variables of our model are α, β_{\pm} . This model is reduced to closed FRW model when $\beta_{\pm} = 0$. The (Lorentzian) action of this model is calculated to be

$$S = \frac{\pi}{G} \int dt N e^{3\alpha} \left[\frac{6}{N^2} (-\dot{\alpha}^2 + \dot{\beta}_+^2 + \dot{\beta}_-^2) + {}^3R_{\text{IX}} \right] \quad (5)$$

where we do not include cosmological constant at the moment, the three-curvature ${}^3R_{\text{IX}}$ is

$$\begin{aligned} {}^3R_{\text{IX}} &= \frac{1}{2} e^{-2\alpha} \text{tr}(2e^{-2\beta} - e^{4\beta}) \\ &= e^{-2\alpha} [2e^{-2\beta_+} \cosh 2\sqrt{3}\beta_- \\ &\quad - \frac{1}{2} e^{-8\beta_+} + e^{4\beta_+} (1 - \cosh 4\sqrt{3}\beta_-)] \\ &\equiv -\frac{1}{2} e^{-2\alpha} V(\beta_+, \beta_-) \end{aligned}$$

Then the Hamiltonian for the Bianchi type IX universe is

$$H_{\text{IX}} = \frac{GN}{24\pi} e^{-3\alpha} [-p_\alpha^2 + p_+^2 + p_-^2 + \frac{12\pi^2}{G^2} e^{4\alpha} V(\beta_+, \beta_-)] \quad (6)$$

The conjugate momenta of α and β_{\pm} are as follows.

$$p_\alpha = -\frac{12\pi}{GN} e^{3\alpha} \dot{\alpha} \quad (7)$$

$$p_{\pm} = \frac{12\pi}{GN} e^{3\alpha} \dot{\beta}_{\pm} \quad (8)$$

It is possible to think the Hamiltonian (6) as that of a particle with triangular shaped potential $V(\beta_+, \beta_-)$ whose walls are very steep. Therefore the evolution of the closed universe with anisotropy may be expressed by the motion of this point mass (e.g. Misner, Thorne & Wheeler [8]). Since the motion of the point shows chaotic behavior in general by bouncing between potential walls, it is argued that the classical universe is predicted to behave chaotically taking all possible values of anisotropies. This model of the universe is called the mixmaster universe .

III. NO BOUNDARY WAVE FUNCTION OF THE UNIVERSE AND SEMI-CLASSICAL APPROXIMATION

In this section we review the semi-classical approximation of the no-boundary wave function of the universe according to HHH.

The no-boundary wave function is defined by sum-over-histories

$$\Psi[\hat{q}^A] = \int \delta q^A \exp(-I[q^A(\lambda)]/\hbar) \quad (9)$$

where $q^A(\lambda)$ are histories of dynamical variables such as a, β_{\pm} , etc, and $I[q^A(\lambda)]$ is their Euclidean action. The sum is carried out over cosmological geometries that are regular on a manifold with only one boundary at which $q^A(\lambda)$ take some prescribed real values. The integration is carried out along a suitable complex contour which ensures the convergence of the integral and the reality of the result.

We use the steepest descent approximation to evaluate the path integral. We consider only paths that extremize the action.

$$\frac{\delta I}{\delta q^A(\lambda)} = 0 \quad (10)$$

then we can write

$$\Psi(\hat{q}^A) = \sum_{\text{ext}} \exp[-\mathcal{A}_{\text{ext}}/\hbar] \quad (11)$$

where the summation run over the extrema. The equations given by (10) are recognized as Euclidean Einstein equations. Note that these extremized paths are complex contours, not real with a few exceptions (Halliwell and Hartle [9]). Of course the physical quantities are real,

thus we will set the boundary value \hat{q}^A as real. Therefore the extremized paths are *fuzzy instanton*, which started as complex Euclidean geometry and growing to asymptotically real Lorentzian at large scale.

We consider only the lowest order in \hbar , thus

$$\begin{aligned}\mathcal{A}_{\text{ext}} &= I_{\text{ext}}(q^A) + O(\hbar) \\ &\equiv I[q_{\text{ext}}^A(\lambda)] + O(\hbar)\end{aligned}\quad (12)$$

From now we drop the subscript 'ext'. Since the Euclidean action is complex, we can divide the action into real part and imaginary part, $I = I_R - iS$ and write the wave function as follows;

$$\begin{aligned}\Psi(\hat{q}^A) &= A(q^A)e^{iS(q^A)/\hbar} \\ A(q^A) &\equiv e^{-I_R(q^A)/\hbar}\end{aligned}\quad (13)$$

The wave function is said to be the approximate semi-classical form when $S(q^A)/\hbar$ varies rapidly and $A(q^A)$ varies slowly. Then the wave function in this region of minisuperspace predicts an ensemble of classical trajectories. Therefore

$$|\nabla_A I_R| \ll |\nabla_A S| \quad (14)$$

is called the *classicality condition*. Using conserved current

$$J_A \equiv -\frac{i\hbar}{2} \left(\Psi^* \frac{\partial \Psi}{\partial q^A} - \Psi \frac{\partial \Psi^*}{\partial q^A} \right) \quad (15)$$

we assume that the relative probability density of classical history is the component of the conserved current along the specific surface in minisuperspace.

$$\begin{aligned}\rho(q^A) &\equiv J \cdot n = |A(q^A)|^2 \nabla_n S(q^A) \\ &= e^{-2I_R(q^A)} \nabla_n S\end{aligned}\quad (16)$$

n is the normal of the spacelike surface in minisuperspace. If we get the complex paths which extremize the Euclidean action and satisfy the classicality condition, we are able to calculate the classical Lorentzian history by using these paths as initial condition.

$$\begin{aligned}S_{\text{Lorentz}}(q_L^A) &= -\text{Im}[I(\hat{q}^A)] \\ q_L^A &= \hat{q}^A \\ p_L^A &= -\text{Im}(p^A)\end{aligned}\quad (17)$$

Summarize this section

STEP1

Calculate equation (10) to get the Euclidean Einstein equations.

STEP2

Solve these equations in complex plane under the condition that the boundary values are real.

STEP3

Check whether the solutions satisfy the classicality condition (14) or not.

STEP4

Solve the classical Lorentzian paths and calculate the relative probabilities of these histories.

IV. NO-BOUNDARY WAVE FUNCTION FOR MIXMASTER UNIVERSES

In this section we calculate the steepest descent approximation to the no-boundary wave function for the mixmaster universes according to the above prescriptions. We include the cosmological constant and a minimally coupled single scalar field with quadratic potential.

By replacing $t \rightarrow -i\lambda$, $iS \rightarrow -I$ in (5), the Euclidean action becomes

$$I[a(\lambda), \Phi(\lambda), \beta_{\pm}(\lambda)] = I_{\text{IX}} + I_{\Phi} \quad (18)$$

where I_{IX} is the action of spacetime

$$I_{\text{IX}} = \frac{\pi}{G} \int d\lambda N e^{3\alpha} \left[\frac{6}{N^2} (-\alpha'^2 + \beta_+'^2 + \beta_-'^2) - {}^3R_{\text{IX}} + 2\Lambda \right] \quad (19)$$

with $A' = dA/d\lambda$. I_{Φ} is the action for the minimally coupled scalar field with a quadratic potential

$$\begin{aligned}I_{\Phi} &= \int d^4x \sqrt{-g} \mathcal{L}_{\text{matter}} \\ &= (4\pi)^2 \int d\lambda N e^{3\alpha} \left[\frac{1}{2N^2} \Phi'^2 - \frac{1}{2} m^2 \Phi^2 \right]\end{aligned}\quad (20)$$

We have assumed that scalar field is homogeneous, and m is the mass of scalar field. For later convenience, we rescale the variables as follows;

$$e^{\alpha} = a \quad (21)$$

$$N \rightarrow \sqrt{\frac{3}{\Lambda}} N \quad (22)$$

$$a \rightarrow \frac{1}{2} \sqrt{\frac{3}{\Lambda}} a \quad (23)$$

$$\Phi = \sqrt{\frac{3}{4\pi G}} \phi \quad (24)$$

$$m = \sqrt{\frac{\Lambda}{3}} \mu \quad (25)$$

Then the explicit form of the Euclidean action takes the following form

$$\begin{aligned}
I[a(\lambda), \Phi(\lambda), \beta_{\pm}(\lambda)] &= \frac{9\pi}{4\Lambda G} \int_0^1 d\lambda N a^3 \left[\frac{1}{N^2} \left(-\frac{a'^2}{a^2} + \beta_+'^2 + \beta_-'^2 \right) \right. \\
&\quad \left. + 1 - \frac{1}{a^2} (1 - V(\beta_{\pm})) + \frac{\phi'^2}{N^2} + \mu^2 \phi^2 \right] \quad (26)
\end{aligned}$$

where

$$\begin{aligned}
V(\beta_{\pm}) &= 1 - \frac{4}{3} e^{-2\beta_+} \cosh 2\sqrt{3}\beta_- \\
&\quad + \frac{1}{3} e^{-8\beta_+} - \frac{2}{3} e^{4\beta_+} (1 - \cosh 4\sqrt{3}\beta_-) \quad (27)
\end{aligned}$$

Note that the variables are all complex valued. Therefore the parameter λ can be chosen to be real, and we choose $\lambda = 0$ at the starting point and $\lambda = 1$ is our boundary.

Taking the variation to the above Euclidean action and using the new complex parameter $d\tau = Nd\lambda$, we get five equations

$$\begin{aligned}
\dot{a}^2 - a^2(\dot{\beta}_+^2 + \dot{\beta}_-^2) \\
+ a^2 - (1 - V(\beta_{\pm})) + a^2 \dot{\phi}^2 + a^2 \mu^2 \phi^2 = 0 \quad (28)
\end{aligned}$$

$$\begin{aligned}
\ddot{a} + \frac{\dot{a}^2}{2a} + \frac{3}{2} a(\dot{\beta}_+^2 + \dot{\beta}_-^2) \\
- \frac{1}{2a} (1 - V(\beta_{\pm})) + \frac{3}{2} a(\dot{\phi}^2 + \mu^2 \phi^2) = 0 \quad (29)
\end{aligned}$$

$$\ddot{\phi} + 3\frac{\dot{a}}{a}\dot{\phi} - \mu^2 \phi = 0 \quad (30)$$

$$\ddot{\beta}_{\pm} + 3\frac{\dot{a}}{a}\dot{\beta}_{\pm} - \frac{1}{2a^2} \frac{\partial V(\beta_{\pm})}{\partial \beta_{\pm}} = 0 \quad (31)$$

where $\dot{A} = dA/d\tau$. Four in the above five equations are independent. Finally, the Euclidean action is written as

$$\begin{aligned}
I[a(\tau), \phi(\tau), \beta_{\pm}(\tau)] &= \frac{9\pi}{4\Lambda G} \int_{C(0,v)} d\tau \left[a\dot{a}^2 + a^3(\dot{\beta}_+^2 + \dot{\beta}_-^2) \right. \\
&\quad \left. + a^3 - a(1 - V(\beta_{\pm})) + a^3 \dot{\phi}^2 + \mu^2 a^3 \phi^2 \right] \\
&= \frac{9\pi}{2\Lambda G} \int_{C(0,v)} d\tau a [a^2(1 + \mu^2 \phi^2) - 1 + V(\beta_{\pm})] \quad (32)
\end{aligned}$$

Note that the action is given by line integral over the contour in complex τ -plane, $C_{(0,v)}$, start from origin to $v = X + iY$. Following Lyons [10], we integrate along the real axis to X first, and then along the imaginary axis to $v = X + iY$ where the variables are asymptotic real.

At the initial position $\tau = 0$, we require that the scale factor $a(0) = 0$ and all other variables are regular. Thus

we can Taylor expand the variables near the origin $\tau = 0$ and get the following expressions

$$a(\tau) = \tau - \frac{1}{6} (1 + \mu^2 \bar{\phi}_0^2) \tau^3 + O(\tau^5) \quad (33)$$

$$\begin{aligned}
\phi(\tau) &= \bar{\phi}_0 + \frac{1}{8} \mu^2 \bar{\phi}_0 \tau \\
&\quad + \frac{1}{48} \mu^2 \bar{\phi}_0 (2 + \mu^2 + 2\mu^2 \bar{\phi}_0^2) \tau^3 + O(\tau^5) \quad (34)
\end{aligned}$$

$$\begin{aligned}
\beta_+(\tau) &= \bar{P}_2 \tau^2 \\
&\quad + \left[\frac{7}{24} (1 + \mu^2 \bar{\phi}_0^2) \bar{P}_2 - 10\bar{P}_2^2 + 10\bar{M}_2^2 \right] \tau^4 \\
&\quad + O(\tau^6) \quad (35)
\end{aligned}$$

$$\begin{aligned}
\beta_-(\tau) &= \bar{M}_2 \tau^2 \\
&\quad + \left[\frac{7}{24} (1 + \mu^2 \bar{\phi}_0^2) \bar{M}_2 + 5\bar{P}_2 \bar{M}_2 \right] \tau^4 + O(\tau^6) \quad (36)
\end{aligned}$$

This shows that we can choose three complex numbers $\bar{\phi}_0, \bar{P}_2, \bar{M}_2$ as our free parameters. We write them as follows:

$$\bar{\phi}_0 = |\bar{\phi}_0| e^{i\theta} \equiv \phi_0 e^{i\theta} \quad (37)$$

$$\bar{P}_2 = |\bar{P}_2| e^{i\Theta_p} \equiv P_2 e^{i\Theta_p} \quad (38)$$

$$\bar{M}_2 = |\bar{M}_2| e^{i\Theta_m} \equiv M_2 e^{i\Theta_m} \quad (39)$$

V. RESULTS

A. COMPLEX SOLUTION

We now solve the complex Einstein's equations with the condition that the imaginary part of the dynamical variables become zero at large τ .

Figure.1 and Figure.2 show the real and imaginary part of the scale factor a , scalar field ϕ , anisotropy β_{\pm} . The parameters are $\mu = 3/4$, $\phi_0 = 2$, $P_2 = 0.02$, and $M_2 = 0.15$. If $P_2 = M_2 = 0$, the parameters are same as HHH's model. All imaginary parts become zero at large scale as seen by these figures.

Figure.3 shows the real part of β_+ vs β_- in the triangular-shaped potential. We can see that the universe point bounces between steep walls of the potential. However, note that this is an Euclidean solution and not directly corresponds to the classical history. In fact, the corresponding Lorentzian history has completely different trajectory, see Figure.6.

The real and imaginary parts of the Euclidean action are shown in Figure.4. While the real part of the action is oscillating in $y < 1$, the real part stabilizes and imaginary part is rapidly varying in $y > 2$ (in large scale). This solution satisfies the classicality condition (14), thus there exist a corresponding classical Lorentzian history. The real part of Euclidean action provides the relative

probability of history.

$$\rho(q^A) = e^{-2I_R(q^A)} \nabla_n S$$

In Figure.4, the real part of action stabilizes at $I_R \sim 0.5$. In the isotropic model, $I_R \sim -0.1$. We can see that the probability of the anisotropic universe is less than that of isotropic one.

B. CLASSICAL LORENTZIAN SOLUTIONS

Next, we calculate the Lorentzian histories by using the complex solution as initial condition.

Figure.5 shows the two Lorentzian histories. One (we call model A) has large anisotropy, the another (model B) has small anisotropy. If there is no anisotropy, the history shows initial bouncing behavior as shown by HHH. Similarly, model B is bouncing as in isotropic case. On the other hand, model A has an initial singularity. Usually, the existence of singularity is regarded as a sign of the breakdown of the theory. However HHH claimed that the no-boundary wave function predicts the probability of classical *histories* rather than initial data, thus the initial singularity is not a signal of break down of the theory. Since the second time derivative of the scale factor d^2a/dt^2 is positive in both models, these histories have inflationary period.

The motion of anisotropy in triangular-shaped potential is shown in Figure.6. Model A has started with high anisotropy, and then rolled down to narrow valley, and arrived at low anisotropic state. Model B has started at the bottom area of potential, and wandering around the initial position. In both models, the anisotropy will approach to constant value at large scale, and nearly vanishes. These features are consistent with preceding studies (e.g. Hawking and Luttrell [11], Wright and Moss [12] etc.).

The real part of the Euclidean action is shown in Figure.7. The figure clearly shows that the probability of high anisotropic histories are smaller than low anisotropic histories. Model B's probability is slightly smaller than isotropic one.

Figure.8 shows the area where the classical histories exist in $P_2 - M_2$ plane. We do not change μ, ϕ_0 . White points represent the histories with initial bounce, and black points represent histories with initial singularity. Clearly we can see that there is the critical line where the initial state changed drastically, the high values of P_2, M_2 area have initial singularity. Note that P_2, M_2 are the absolute values of *second differential* of β_+, β_- in initial condition, not the initial value. We could not find the solution outside of the plotted area. There seems to be an upper limit in each P_2, M_2 .

The relative probability distribution is shown in Figure.9. The probability has maximum at isotropic history,

and is rapidly decreasing with the increase of anisotropy. Figure.10 shows the distribution of β_+, β_- at the bounce, and Figure.11 shows their probability distribution. We can see that states with low anisotropies have higher probabilities.

We found that the distribution of the anisotropy near the bounce is highly inhomogeneous. This is very different from classical result. While the classical result predicts chaotic behavior near the initial singularity [13][14], we could not see such a behavior.

The anisotropy at large scale are shown in Figure.12 and Figure.13. Clearly, the probability is peaked around the isotropic history. Therefore *the no-boundary wave function of the universe predicts nearly isotropic universe*.

VI. CONCLUSION & DISCUSSION

We investigated the emergence of the classical Mix-master universe with a single scalar field and with the cosmological constant from the no-boundary quantum state according to the method of HHH. We confirmed that there are complex solutions that satisfy the classicality condition, thus there are classical Lorentzian histories with any amount of anisotropies. This fact implies that the method of HHH can be applied for a wide range of models. It is also found that the probability of anisotropic universe is lower than isotropic one. In addition the emerged classical universe experiences the inflationary expansion and the remaining anisotropy decreases rapidly. Thus the quantum cosmology with no-boundary wave function may be able to explain quite naturally the emergence of our universe.

We also found that the classical histories have initial singularity or initial bounce depending on the initial acceleration of anisotropies. High acceleration may induce the initial singularity. The no-boundary proposal seems to predict that the distribution of anisotropy near the bounce or singularity is not homogeneous and very different from the prediction by classical theory and by analysis of Wheeler-DeWitt equation [7]. On the other hand, the loop quantum cosmology predicts non-chaotic behavior near singularity [15]. Thus it would be very interesting to see if the non-chaotic behavior is general in more general spacetimes.

Acknowledgments

We thank S. Yoshida for useful advices of numerical calculation. This work is supported in part by a Grants-in-Aid for Scientific Research from JSPA(Nos. 1807200, 20540245) as well as by Core-to-Core Program "International Research Network for Dark Energy".

-
- [1] A.Vilenkin, Phys. Rev. D,37,888 (1988)
 - [2] A. Ashtekar. 2007NCimB.122,135A
 - [3] M. Bojowald, LivingRev. Rel.8, 11, (2005)
 - [4] J.B. Hartle and S.W. Hawking, Phs. Rev. D,28,2960H (1983)
 - [5] S.W. Hawking, Nucl. Phys. B,239,257-276 (1984)
 - [6] J.B. Hartle, S.W. Hawking, and T.Hertog, Phys. Rev. D,77,123537 (2008)
 - [7] M.V. Battisti, R. Belvedere, and G. Montani, arXiv 0903.3837V (2009)
 - [8] C.W. Misner, K.S. Thorne, and J.A. Wheeler, W H Freeman & Co (1973)
 - [9] J.J. Halliwell and J.B. Hartle, Phs. Rev. D,41,1815H (1990)
 - [10] G.W. Lyons, Phs. Rev. D,46,1546L (1992)
 - [11] S.W. Hawking and J.C. Luttrell, Phys. Lett. B,143B (1984)
 - [12] W.A. Wright and I.G. Moss, Phys. Lett. B,vol.154B (1984)
 - [13] C.W. Misner, Phys. Rev. Lett.22, 1071 (1969)
 - [14] V. A. Belinskii, I. M. Khalatnikov, and E. M. Lifshitz, Adv. Phs. 19, 525 (1970)
 - [15] M. Bojowald, G. Date and G.M. Hossan, Class. Quant. Grav. 21, 3541 (2004)
 - [16] W.G. Unruh and M. Jheeta, arXiv:gr-qc/9812017
 - [17] T. Furusawa, 1986PThPh.75.59F and 76.67F

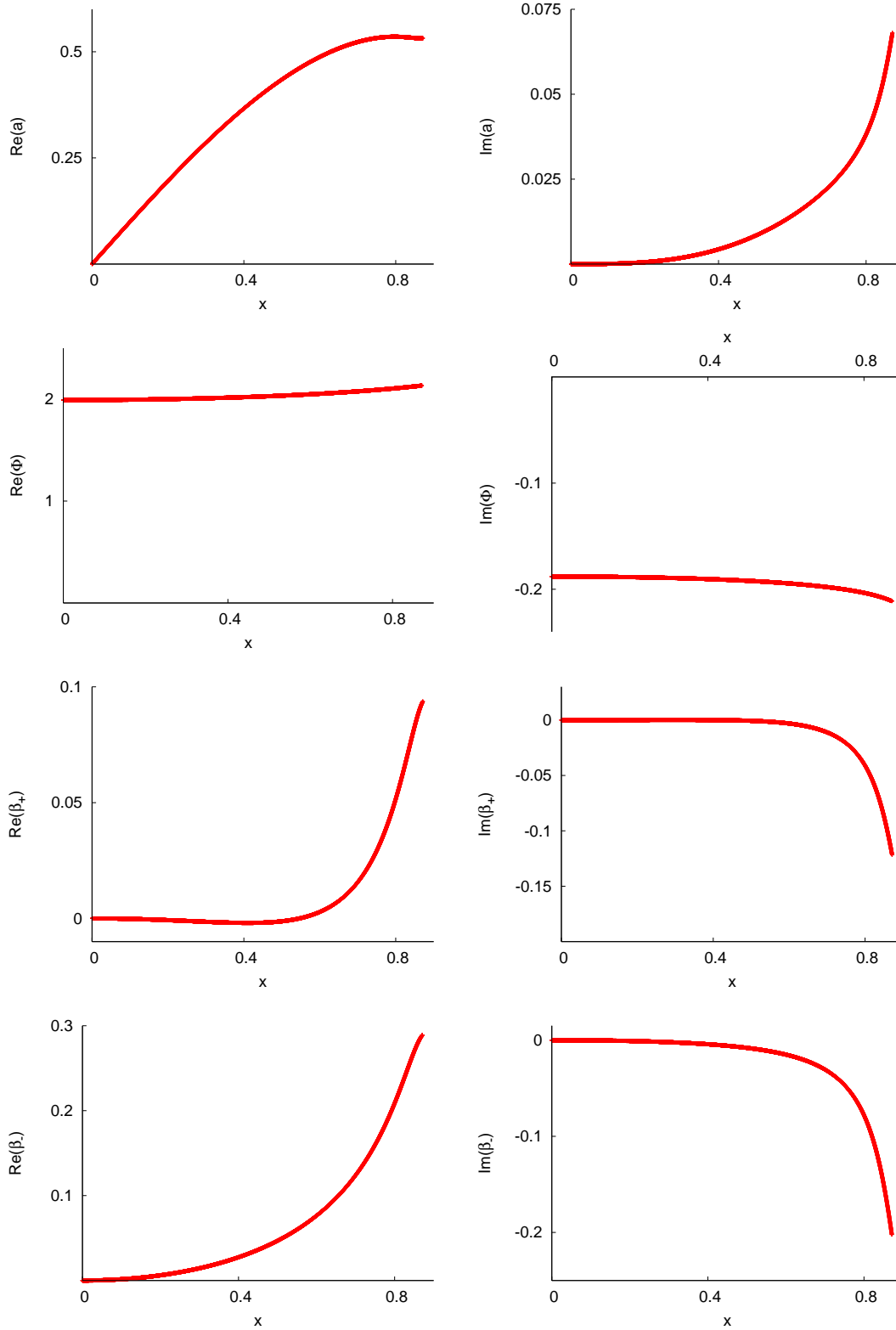


FIG. 1: The real and imaginary part of the complex-Euclidean solution on X-axis.

From top to bottom, scale factor a , scalar field ϕ , anisotropy β_+ and β_- .

Left row are real part, right row are imaginary part of the variables.

$\mu = 3/4$, $\phi_0 = 2$, $P2 = 0.02$, $M2 = 0.15$ and $X = 0.871$, $\theta = 0.0942$, $\Theta_p = 3.01$, $\Theta_m = -0.133$

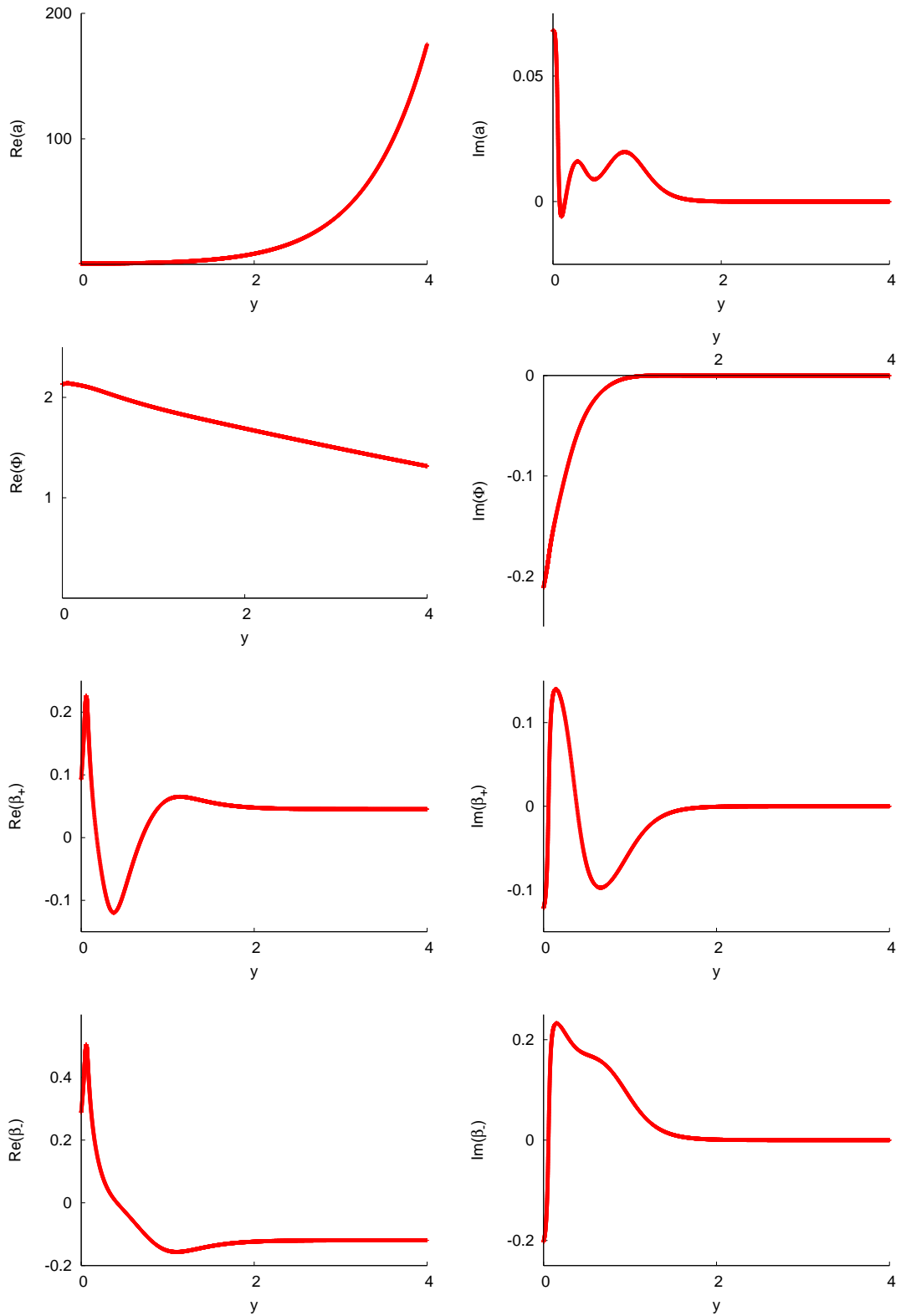


FIG. 2: The real and imaginary part of the complex-Euclidean solution on Y-axis
All imaginary parts become zero at large scale.

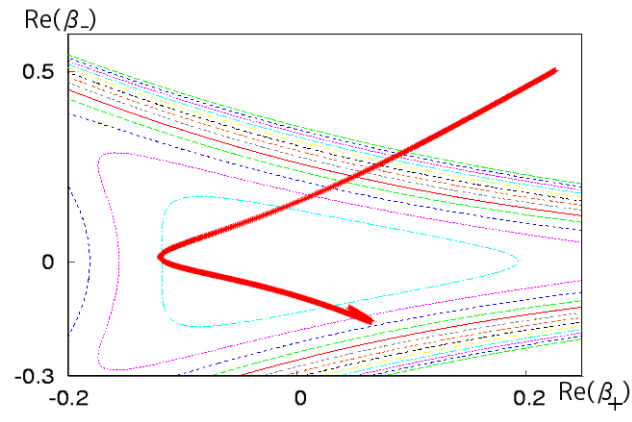


FIG. 3: The real part of β_+ vs β_- .
The universe point comes from high anisotropy to low anisotropy with some bounce.
Note that this is in Euclidean solution, not classical Lorentzian.

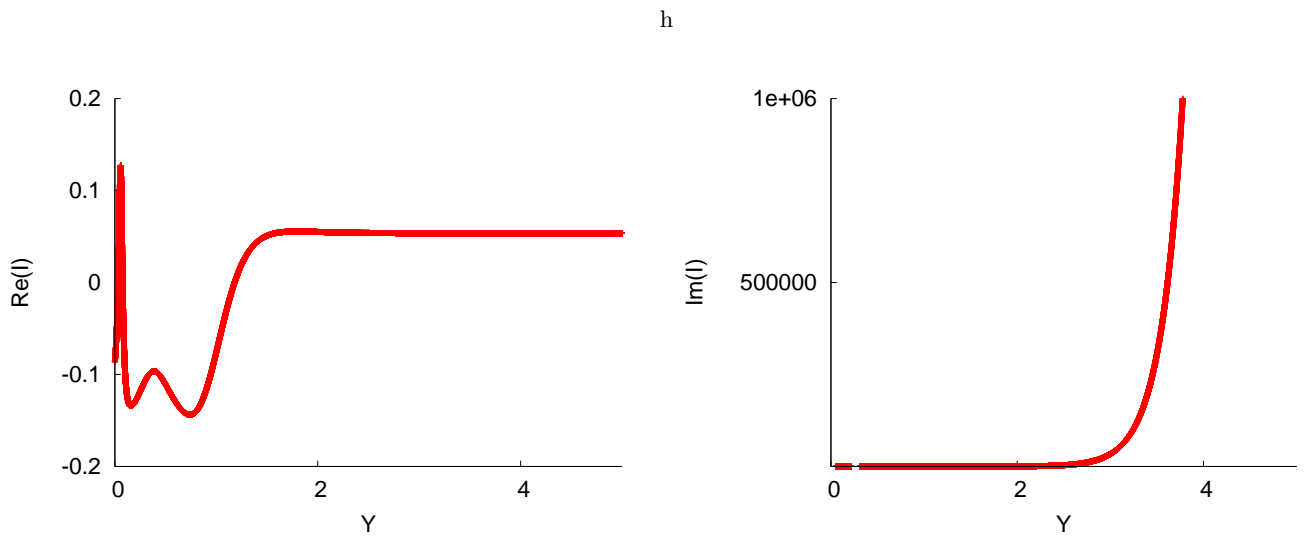


FIG. 4: The real and imaginary part of the Euclidean action I .

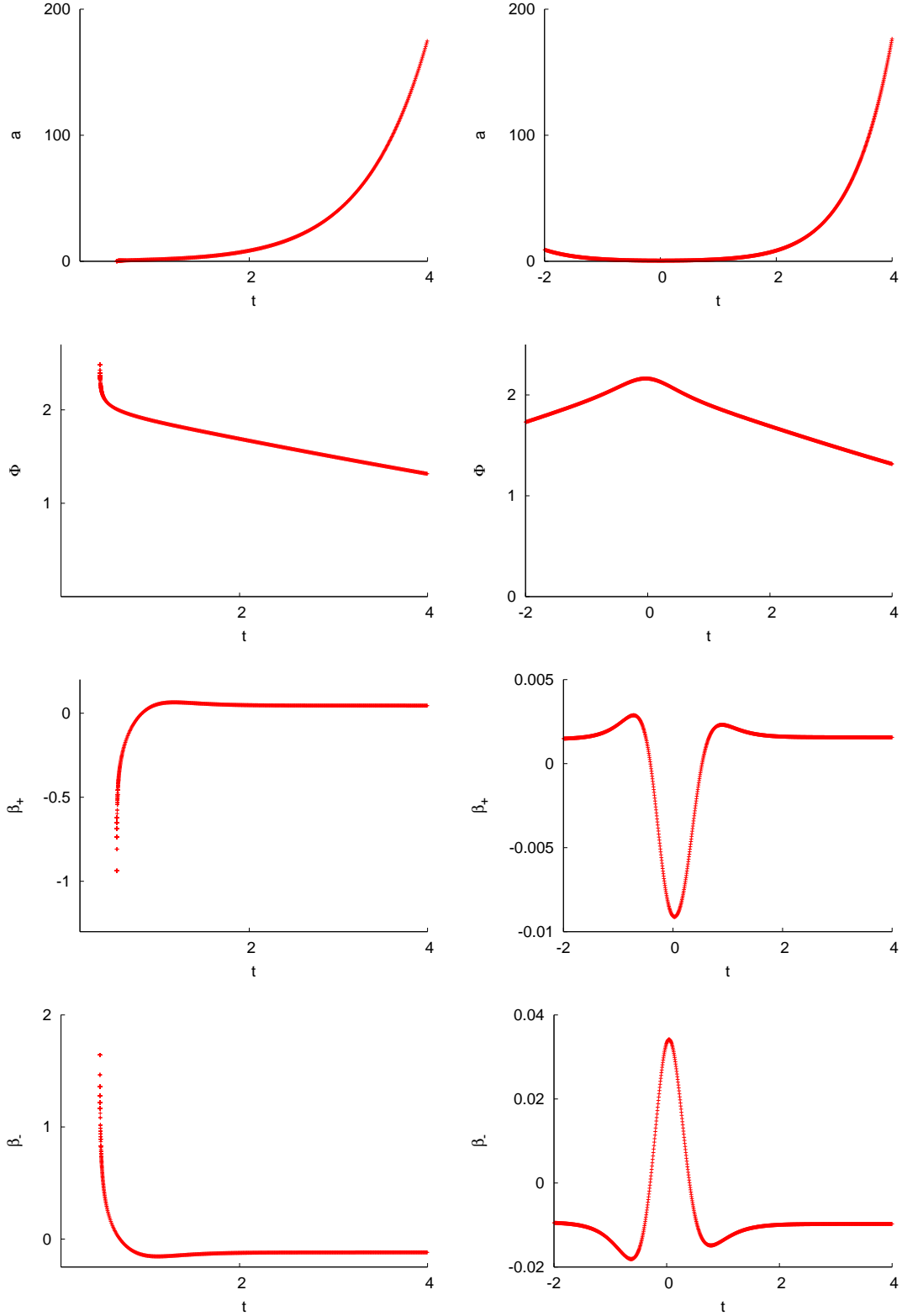


FIG. 5: Lorentzian history of two models. From top to bottom, a , ϕ , β_+ , β_- .
 Left row is model A (high anisotropy), right row is model B (little anisotropy).
 We use the complex Euclidean solution at $Y = 4$ as initial value at $t = 4$.
 Model A: $\mu = 3/4$, $\phi_0 = 2$, $P2 = 0.02$, $M2 = 0.15$
 Model B: $\mu = 3/4$, $\phi_0 = 2$, $P2 = 0.002$, $M2 = 0.015$

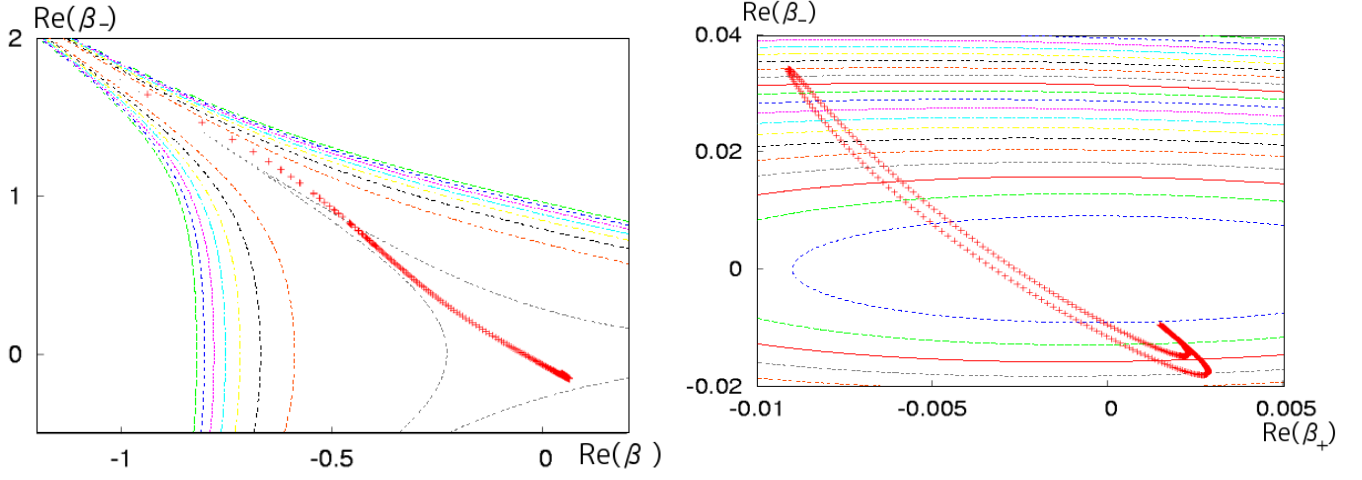


FIG. 6: β_+ vs β_- in classical history. Left is model A, right is model B.

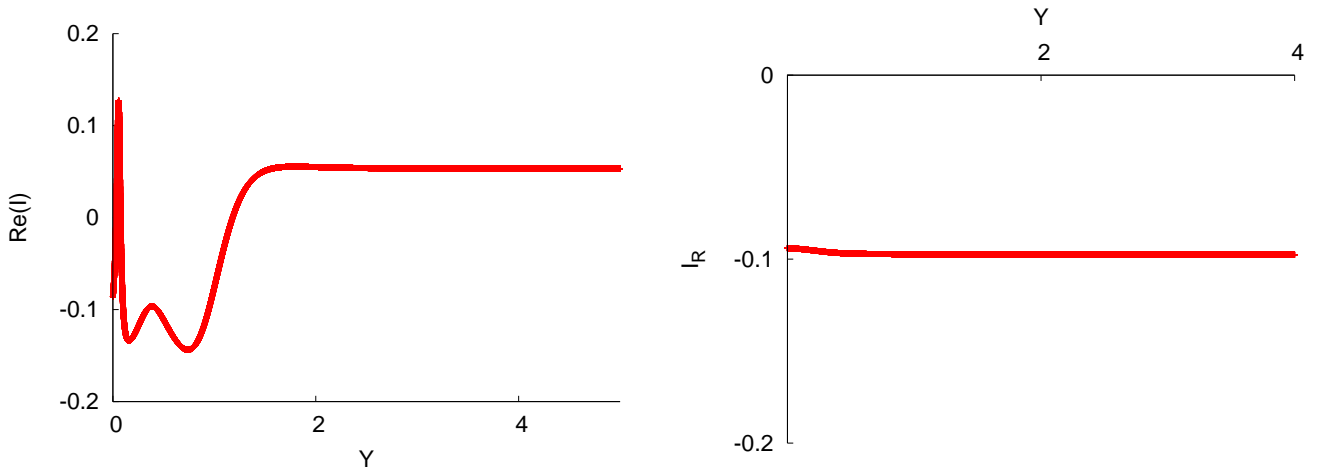


FIG. 7: The real part of the Euclidean action. Left is model A, right is model B. The probability of model A is smaller than model B.

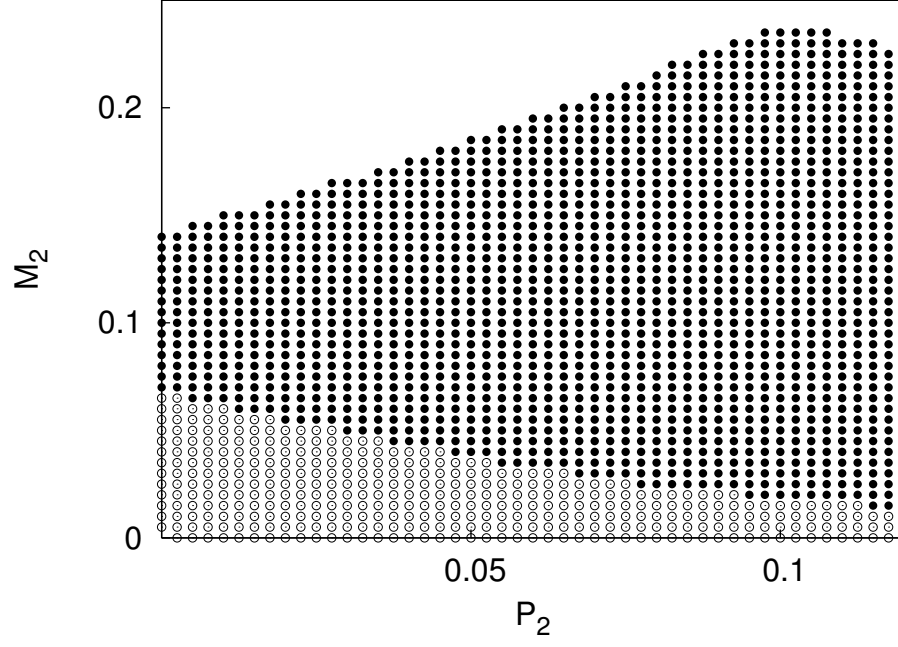


FIG. 8: The area where the classical histories exist in $P_2 - M_2$ plane. White points represents the histories which has initial bounce, black ones has initial singularity. There is critical line where the initial state changed and upper limits.

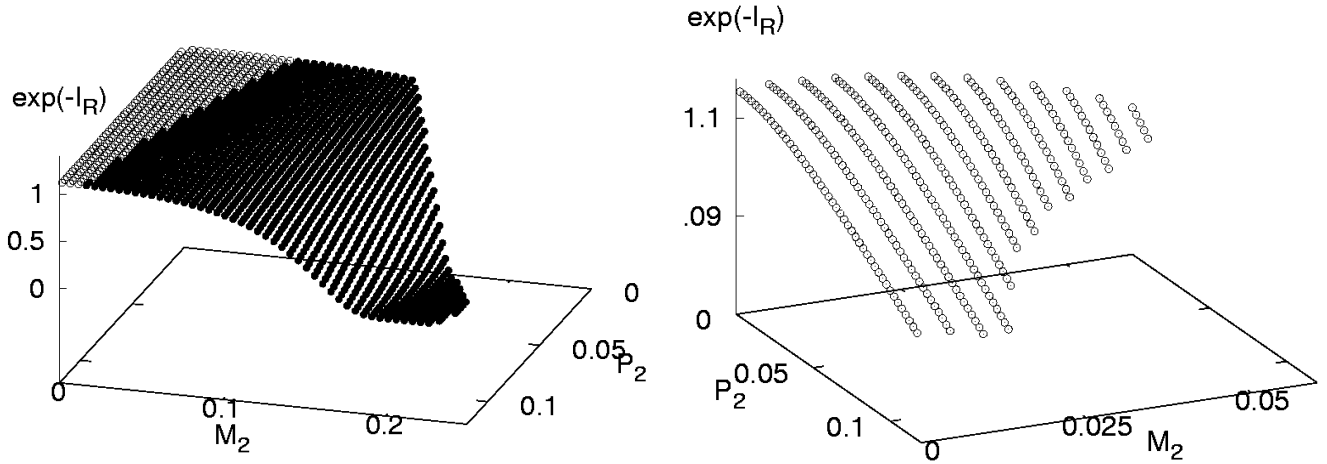


FIG. 9: The relative probability distribution in $P_2 - M_2$ plane. Left represents same area with Fig.8, right represents the area nearby origin (Isotropic).

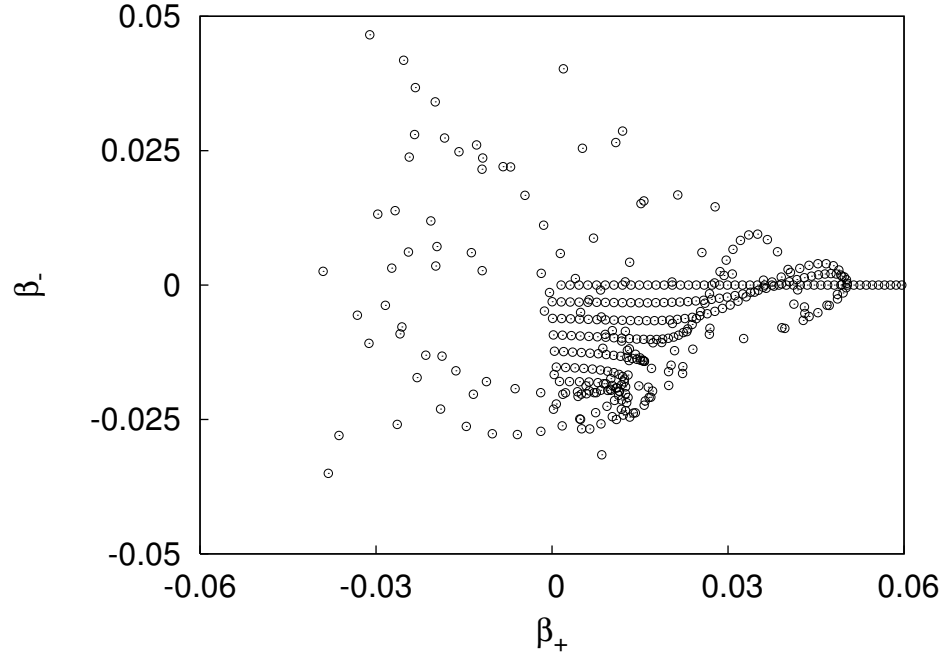


FIG. 10: β_+ vs β_- at the bounce.

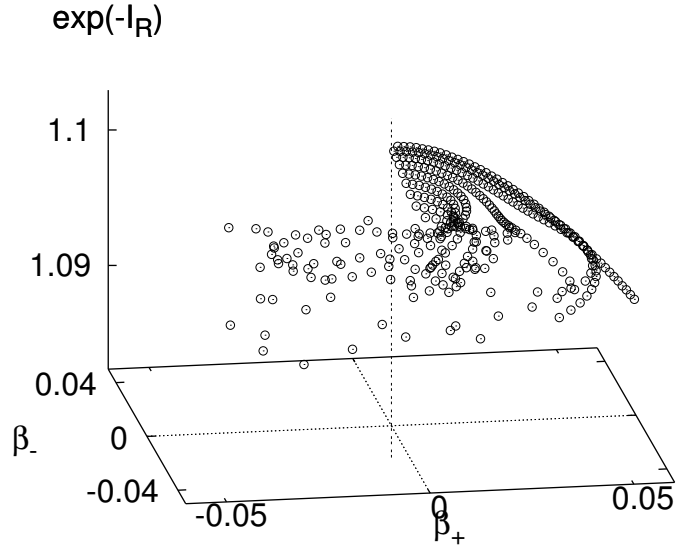


FIG. 11: The relative probability distribution in $\beta_+ - \beta_-$ plane at the bounce. There is high probability surface but no clear structure at low probability.

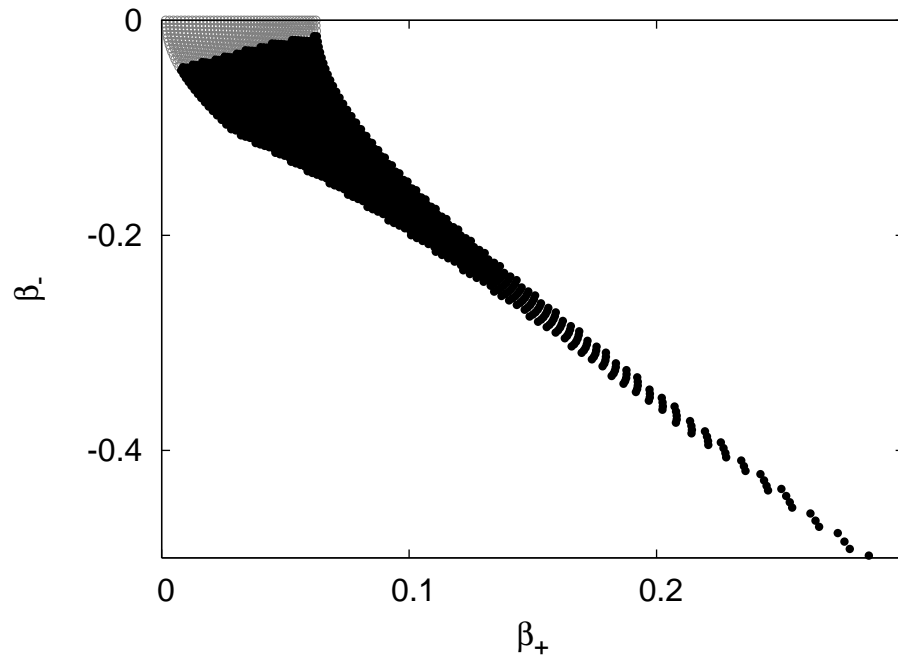


FIG. 12: β_+ vs β_- at large scale in classical history. White region represents bouncing history, black region has initial singularity. Since the anisotropy is constant at large scale (see Fig. 5), this figure represents the observable one.

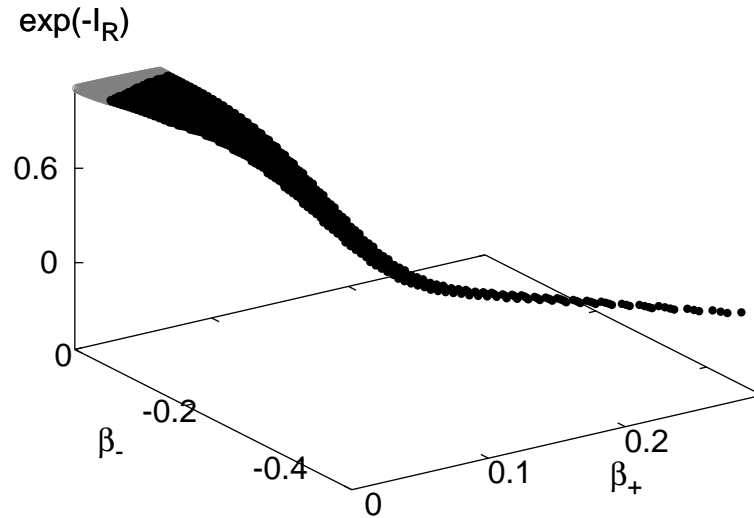


FIG. 13: The relative probability distribution in $\beta_+ - \beta_-$ at large scale in classical history. The probability distribution is peaked around the isotropic universe.